IceBridge BedMachine Greenland, Version 4

USER GUIDE

How to Cite These Data

As a condition of using these data, you must include a citation:

Morlighem, M. et al. 2021. *IceBridge BedMachine Greenland, Version 4*. [Indicate subset used]. Boulder, Colorado USA. NASA National Snow and Ice Data Center Distributed Active Archive Center. https://doi.org/10.5067/VLJ5YXKCNGXO. [Date Accessed].

Literature Citation

As a condition of using these data, we request that you acknowledge the author(s) of this data set by referencing the following peer-reviewed publication.

Morlighem, M., C. Williams, E. Rignot, L. An, J. E. Arndt, J. Bamber, G. Catania, N. Chauché, J. A. Dowdeswell, B. Dorschel, I. Fenty, K. Hogan, I. Howat, A. Hubbard, M. Jakobsson, T. M. Jordan, K. K. Kjeldsen, R. Millan, L. Mayer, J. Mouginot, B. Noël, C. O'Cofaigh, S. J. Palmer, S. Rysgaard, H. Seroussi, M. J. Siegert, P. Slabon, F. Straneo, M. R. van den Broeke, W. Weinrebe, M. Wood, and K. Zinglersen. 2017. BedMachine v3: Complete bed topography and ocean bathymetry mapping of Greenland from multi-beam echo sounding combined with mass conservation, *Geophysical Research Letters*. 44. https://doi.org/10.1002/2017GL074954.

FOR QUESTIONS ABOUT THESE DATA, CONTACT NSIDC@NSIDC.ORG

FOR CURRENT INFORMATION, VISIT https://nsidc.org/data/IDBMG4

TABLE OF CONTENTS

1 DETAILED DATA DESCRIPTION

1.1 Format

The data are stored in one netCDF (`.nc`) file named `BedMachineGreenland-2021-04-20.nc`.

1.2 Spatial Coverage

Spatial coverage for this data set currently includes Greenland and the Arctic.

Greenland/Arctic:

Southernmost Latitude: 60° N

Northernmost Latitude: 90° N

Westernmost Longitude: 80° W

Easternmost Longitude: 10° E

1.2.1 Spatial Resolution

The output product is generated at 150 m resolution. The true resolution varies between 150 m and 5 km.

1.2.2 Projection and Grid Description

ⓘ This data set is nominally provided in EPSG:3413: the NSIDC Sea Ice Polar Stereographic North projection based on WGS 84. However, the tool used to convert latitudes and longitudes to polar stereographic coordinates was based on the Hughes Ellipsoid. As such, the resulting inverse flattening attribute (298.2794050428205) differs slightly from the EPSG:3413, WGS 84 defined value (298.257223563).

The following table provides details about the coordinate system for this data set.

Table 1. Geolocation Details

Geographic coordinate system	WGS 84
Projected coordinate system	WGS 84 / NSIDC Sea Ice Polar Stereographic North
Longitude of true origin	-45° E
Latitude of true origin	70° N
Scale factor at longitude of true origin	1
Datum	WGS 84
Ellipsoid/spheroid	WGS 84

Units	meters
False easting	0
False northing	0
EPSG code	3413
PROJ4 string	+proj=stere +lat_0=90 +lat_ts=70 +lon_0=-45 +k=1 +x_0=0 +y_0=0 +datum=WGS84 +units=m +no_defs
Reference	https://epsg.io/3413

1.3 Temporal Information

The data were collected between 01 January 1993 and 01 October 2020. The nominal year of this data set is 2007.

1.4 Parameter or Variable

1.4.1 Parameter Description

The BedMachine data file contains parameters as described in Table 2.

Table 2. File Parameter and Units

Parameter Name	Description	Units
bed	Bed elevation (bed topography)	Meters
dataid	Data ID number showing what type of data were available to constrain the map for each pixel: (0 = no data available, 1= gimpdem, 2 = radar, 7 = seismic bathymetry, 10 = multibeam bathymetry)	Flag values
errbed	Bed topography/ice thickness error	Meters
geoid	Geoid height above WGS84 Ellipsoid	Meters
mask	Mask (0 = ocean; 1 = ice-free land; 2 = grounded ice; 3 = floating ice; 4 = non-Greenland land)	Flag values (0 - 4)
source	Data source, Mass Conservation/kriging/bathymetry: (0 = none; 1 = gimpdem; 2 = Mass conservation; 3 = synthetic; 4 = interpolation; 5 = hydrostatic equilibrium; 6 = kriging; 7 = RTOPO-2; 8 = gravity inversion; 10+ = bathymetry data)	Flag values (0 - 46)
surface	Ice surface elevation	Meters
thickness	Ice thickness	Meters

x	Projection x coordinate	Meters
y	Projection y coordinate	Meters

1.4.2 Sample Data Record

Figure 1 illustrates Greenland bedrock altitude and ice thickness.

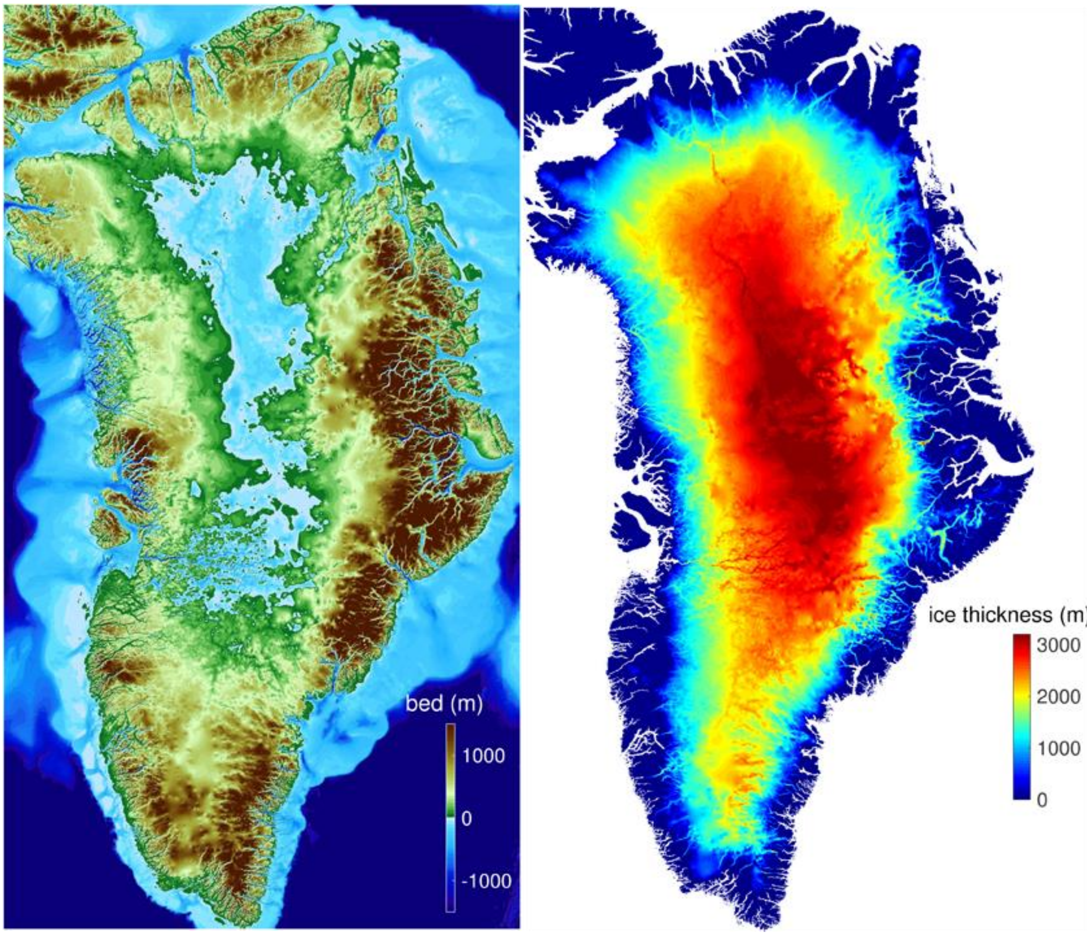

Figure 1. Greenland Bedrock Altitude and Ice Thickness

2 SOFTWARE AND TOOLS

2.1 Software and Tools

See the NetCDF Software Tools web page at NSIDC for tools to view netCDF files.

The netCDF data file is compatible with HDF5 libraries, and can be read by HDF readers such as HDFView. If the netCDF file reader you are using does not read the data, see http://www.unidata.ucar.edu/software/netcdf/ and https://nsidc.org/support/faq/what-netcdf for information on updating the reader.

3 DATA ACQUISITION AND PROCESSING

3.1 Data Acquisition Methods

Source data used in deriving this product include:

- Operation IceBridge radar-derived thickness data, posted at 30 – 60 m, with a vertical precision of 30 m, collected by the MCoRDS radar (IceBridge MCoRDS L2 Ice Thickness; IRMCR2).
- Ice thickness data from the Doppler focused radar of the Technical University of Denmark (DTU) for the region of 79 North (Thomsen et al., 1997; Christensen et al., 2000) and Russell (Lindbäck et al., 2014).
- Ice thickness data from the High CApability Radar Sounder (HiCARS; Peters et al., 2005; Peters et al., 2007) operated by the University of Texas, Institute for Geophysics
- Ice thickness data from the Pathfinder Advanced Radar Ice Sounder (PARIS; Raney, 2010)
- Ice thickness data from the Alfred Wegener Institute (AWI; Nixdorf et al., 1999)
- Ice thickness data from Uppsala University (UU; Lindbäck et al., 2014), collected in the vicinity of Russell Gletscher
- Multibeam echo sounding data from Oceans Melting Greenland (OMG Missions 2016, 2017, and 2020) along the coast of West and Southeast Greenland
- Bathymetry data from Slabon et al. (2016) along the Northwest coast
- Bathymetry data from Weinrebe et al. (2009) in Torssukataq and Uummannaq Fjords
- Bathymetry data from O'Cofaigh et al. (2013) in Uummannaq Fjord
- Bathymetry data from Dowdeswell et al. (2014), Rignot et al. (2015), Fried et al. (2015), and Rignot et al. (2016) in Uummannaq Fjord
- Bathymetry data from Schumann et al. (2012), Holland et al. (2008) and Straneo et al. (2012) in Illulisat Icefjord
- Bathymetry data from Mix et al. (2015) in front of Petermann Fjord and the adjacent Hall Basin
- Bathymetry data from Sutherland et al. (2014) near Kangerdlussuaq

- Bathymetry data from Dowdeswell et al. (2016) in Nordvestfjord
- Bathymetry data from Chauché et al. (2014) near Lille Gletscher
- Bathymetry data from Straneo et al. (2016) in Sermilik fjord
- Bathymetry data from Motyka et al. (2017) in Godthåbsfjord
- Bathymetry data from Stevens et al. (2016) in Sarqardleq fjord
- Bathymetry data from Kjeldsen et al. (2017) in Timmiarmiut Fjord, Heimdal Glacier and Skjoldungen Fjord
- Bathymetry data from Rysgaard et al. (2003) in Young Sound fjord
- Bathymetry data from Bendtsen et al. (2017) near Flade Isblink Ice Cap
- Single beam bathymetry data from Sutherland and Pickart (2008) on the continental shelf along the Southeast coast
- Single beam data from Olex (www.olex.no) and crowd sourced data from fishing and recreational vessels (MaxSea).
- Bathymetry data from An et al. (2019) along the Northwest Greenland coast
- Bathymetry data from Millan et al. (2018) and An et al. (2019) in Southeast Greenland
- Bathymetry data from An et al. (2021) in Northeast Greenland
- Ice velocity measurements derived from satellite radar data collected during 2008-2009, posted at 150 m, with errors of 10 m yr-1 in speed and 1.5° in flow direction (Mouginot et al., 2017):
    - Japanese Advanced Land Observing System (ALOS) PALSAR
    - Canadian RADARSAT-1 SAR
    - German TerraSAR-X
    - European Envisat Advanced SAR (ASAR)
- Radar data from Center for Remote Sensing of Ice Sheets (CReSIS) (2017)
- Radar data from Hiawatha thickness (Kjaer et al. 2018)
- Radar data from the Programme for Monitoring of the Greenland Ice Sheet (PROMICE) (Søren et al. 2019)
- Radar data from East Greenland Ice Core Project (EGRIP) thickness (Franke et al. 2020)

- Radar data from Northeast Greenland Ice Stream (NEGIS) thickness (Jansen et al. 2020)

Ancillary products used include:

- Surface Mass Balance (SMB) averaged for the years 1961 to 1990 downscaled to 1 km with a precision between 7 percent and 20 percent in the ablation zone (Noël et al., 2016; data set available on request to the authors).
- Ice thickening rates from altimetry data differencing between the years 2003 to 2006 (Khan et al., 2014).
- Surface elevation from the Greenland Mapping Project (GIMP) Digital Elevation Model (Howat et al., 2014; https://byrd.osu.edu/research/groups/glacier-dynamics/data/gimpdem).
- Ice and Ocean mask from the Greenland Mapping Project (GIMP) Digital Elevation Model (Howat et al., 2014; https://byrd.osu.edu/research/groups/glacier-dynamics/data/icemask).
- RTopo-2 (Schaffer et al., 2016, https://doi.pangaea.de/10.1594/PANGAEA.856844).

3.2 Derivation Techniques and Algorithms

Sparse, airborne, radar sounding-derived ice thickness data are combined with comprehensive, high-resolution, ice motion derived from satellite interferometric synthetic-aperture radar to calculate ice thickness based on Mass Conservation (MC). The MC method solves the mass conservation equation to derive ice thickness, while at the same time minimizing departure from the original radar-derived ice thickness data. The algorithm conserves mass fluxes while minimizing the departure from the original radar-derived ice thickness data. Ice surface motion provides a physical basis for extrapolating sparse ice thickness data to larger areas with few or no data. The method works best in areas of fast flow, where errors in flow direction are small and the glaciers slide on the bed. In the interior regions, where errors in flow direction are larger, kriging is used to interpolate ice thickness for the 1993 to 2016 data (Morlighem et al., 2014). Beginning with the 2017 data, streamline diffusion was relied on in the interior regions instead of kriging.

Ocean bathymetry is mapped by combining sparse bathymetry measurements from single and multibeam measurements and casts and RTopo-2 (Schaffer et al., 2016).

The algorithm neglects ice motion by internal shear, which is an excellent approximation for fast-flowing glaciers (>100 m yr-1) (Morlighem et al., 2014).

The bed topography is derived by subtracting the ice thickness from the Greenland Mapping Project (GIMP) Digital Elevation Model (https://byrd.osu.edu/research/groups/glacier-dynamics/data/gimpdem).

3.2.1 Version History

On 19 May 2015, the IceBridge BedMachine Greenland data were replaced by Version 2. Version 2 includes improved processing of some basins and adds some Operation IceBridge 2014 data. Heights are now provided with respect to mean sea level, instead of the WGS84 ellipsoid. The geoid is included in an additional field in the data.

On 25 September 2017, the IceBridge BedMachine Greenland data were replaced by Version 3. Version 3 now includes ocean bathymetry all around Greenland based on data from NASA's Ocean Melting Greenland (OMG) and other campaigns of bathymetry measurements. The subglacial bed topography has also been updated by including more ice thickness data and constraining the ice thickness at the ice/ocean interface based on bathymetry data when available.

On 13 May 2021, the IceBridge BedMachine Greenland data were replaced by Version 4. Version 4 incorporates updated radar data to better constrain the ice thickness inland. Multibeam data for ocean bathymetry has been updated to include data from OMG campaigns 2017 and 2020. Bathymetry data has also been added from new gravity inversions. The format of surface, bed, and thickness has been changed to “single”. Streamline diffusion has been implemented in the interior regions instead of kriging for the Version 4 data beginning January 2017.

3.2.2 Errors and Limitations

Sources of error include error in ice velocity direction and magnitude, error in surface mass balance and ice thinning rates.

In a trial setting with unusually dense radar sounding coverage, we report errors in the MC-inferred thickness of 36 m, only slightly higher than that of the original data. In areas less well constrained by radar-derived thickness data, or constrained by only one track of data, for example, in south Greenland, errors may exceed 50 m (Morlighem et al., 2013).

No or very little data were available for some fjords, and uncertainty may be high (>500 m).

An error estimate of the bed elevation and ice thickness is provided in the data set, illustrated in Figure 2.

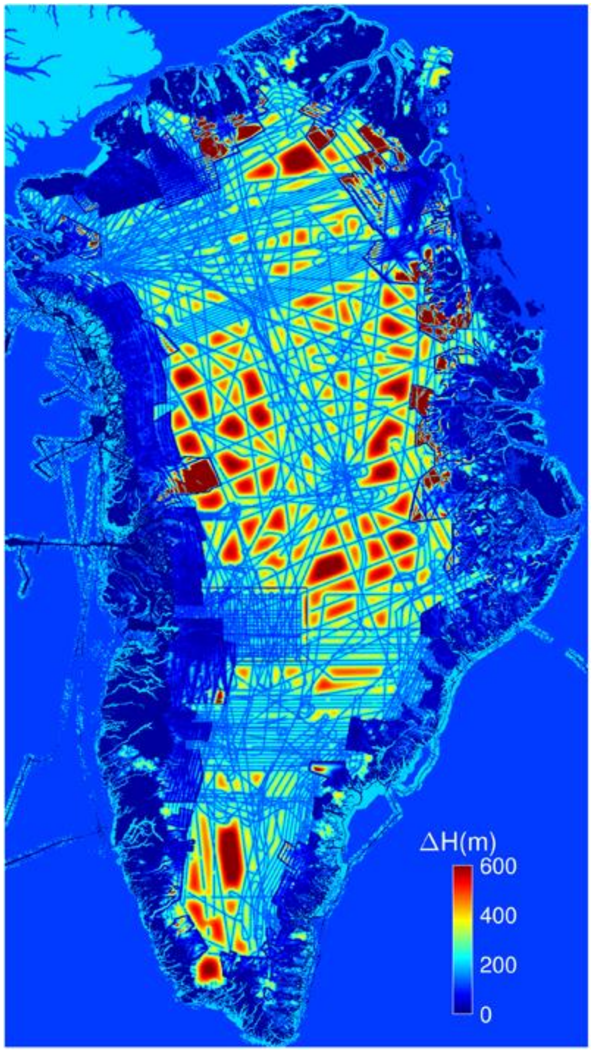

Figure 2. Error Estimate of Greenland Bed Elevation and Ice Thickness

3.3 Sensor or Instrument Description

The Center for Remote Sensing of Ice Sheets (CReSIS) Multichannel Coherent Radar Depth Sounder (MCoRDS) operates over a 180 to 210 MHz frequency range with multiple receivers developed for airborne sounding and imaging of ice sheets. See IceBridge MCoRDS L2 Ice Thickness (IRMCR2) for further information on the MCoRDS radar and the Level-2 data.

4 REFERENCES AND RELATED PUBLICATIONS

An, L., E. Rignot, R. Millan, K. Tinto, and J. Willis. 2019. Bathymetry of northwest Greenland using “Ocean Melting Greenland” (OMG) high-resolution airborne gravity and other data. Remote Sensing, 11(131), doi:10.3390/rs11020131.

An, L., E. Rignot, N. Chauche, D. Holland, D. Holland, M. Jakobsson, et. al. 2019. Bathymetry of southeast Greenland from oceans melting Greenland (OMG) data. Geophysical Research Letters, 46(20):11197– 11205, doi:10.1029/2019GL083953.

An, L., E. Rignot, M. Wood, J. K. Willis, J. Mouginot, S. A. Khan. 2021. Ocean melting of the Zachariae Isstrøm and Nioghalvfjerdsfjorden glaciers, northeast Greenland, Proceedings of the National Academy of Sciences, 118(2):e2015483118, doi:10.1073/pnas.2015483118.

Bendtsen, J., J. Mortensen, K. Lennert, J. K.Ehn, W. Boone, V. Galindo, Y. Hu, I. A. Dmitrenko, S. A. Kirillov, K. K. Kjeldsen, Y. Kristoffersen, D. G.Barber, and S. Rysgaard. 2017. Sea ice breakup and marine melt of a retreating tidewater outlet glacier in northeast Greenland (81°N), Scientific Reports, 7(1), 4941, doi:10.1038/s41598.

Chauché, N., A. Hubbard, J.-C. Gascard, J. E. Box, R. Bates, M. Koppes, A. Sole, P. Christoffersen, and H. Patton. 2014. Ice-ocean interaction and calving front morphology at two west Greenland tidewater outlet glaciers, Cryosphere, 8(4):1457–1468, doi:10.5194/tc-8-1457-2014.

Christensen, E. L., et al. 2000. A low-cost glacier-mapping system, Journal of Glaciology, 46:531.

CReSIS. 2017. Greenland Platform 3 Data, Lawrence, Kansas, USA. Digital Media. http://data.cresis.ku.edu/.

Dowdeswell, J. A., K. A. Hogan, C. O'Cofaigh, E. M. G. Fugelli, J. Evans, and R. Noormets. 2014. Late Quaternary ice flow in a West Greenland fjord and cross- shelf trough system: submarine landforms from Rink Isbrae to Uummannaq shelf and slope, Quat. Sci. Rev., 92(SI), 292–309.

Dowdeswell, J. A., C. L. Batchelor, K. A. Hogan, and H. W. Schenke. 2016. Atlas of Submarine Glacial Landforms: Modern, Quaternary and Ancient, vol. 46, chap. Nord- vestfjord: a major East Greenland fjord system, pp. 43–44, Geological Society, London, Memoirs, doi:10.1144/M46.40.

Ettema, J. et al. 2009. Higher surface mass balance of the Greenland Ice Sheet revealed by high-resolution climate modeling. Geophysical Research Letters, 36:1–5.

Franke, S., D. Jansen, T. Binder, N. Dörr, V. Helm, J. Paden, D. Steinhage, and O. Eisen. 2020. Bed topography and subglacial landforms in the onset region of the Northeast Greenland Ice Stream, Annals of Glaciology, 61(81):143-153, doi:10.1017/aog.2020.12.

Fried, M. J., G. A. Catania, T. C. Bartholomaus, D. Duncan, M. Davis, L. A. Stearns, J. Nash, E. Shroyer, and D. Sutherland. 2015. Distributed subglacial discharge drives significant submarine melt at a Greenland tidewater glacier, Geophys. R, 42(21), 9328– 9336, doi:10.1002/2015GL065806, 2015GL065806.

Holland, D., R. Thomas, B. De Young, M. Ribergaard, and B. Lyberth. 2008. Acceleration of Jakobshavn Isbrae triggered by warm subsurface ocean waters, Nat. Geosci., 1(10), 659–664, doi:10.1038/ngeo316.

Howat, I.M., A. Negrete, B.E. Smith. 2014. The Greenland Ice Mapping Project (GIMP) land classification and surface elevation data sets, The Cryosphere, 8:1509-1518, doi:10.5194/tc-8-1509-2014.

Jakobsson, M., et al. 2012. The International Bathymetric Chart of the Arctic Ocean (IBCAO) Version 3.0, Geophysical Research Letters, 39(12), doi: 10.1029/2012GL052219.

Khan, S. A., K. H. Kjaer, M. Bevis, J. L. Bamber, J. Wahr, K. K. Kjeldsen, A. A. Bjork, N. J. Korsgaard, L. A. Stearns, M. R. van den Broeke, L. Liu, N. K. Larsen, and I. S. Muresan. 2014. Sustained mass loss of the northeast Greenland ice sheet triggered by regional warming, Nat. Clim. Change, 4(4), 292–299, doi:10.1038/nclimate2161.

Kjeldsen, K. K., W. Weinrebe, J. Bendtsen, A. A. Bjørk, and K. H. Kjær. 2017. Multi- beam Bathymetry and CTD-Measurements in two fjord systems in Southeast Greenland, Earth Syst. Sci. Data Disc., 2017, 1–25, doi:10.5194/essd-2017-29.

Lindbäck, K., R. Pettersson, S. H. Doyle, C. Helanow, P. Jansson, S. S. Kristensen, L. Stenseng, R. Forsberg, and A. L. Hubbard. 2014. High-resolution ice thickness and bed topography of a land-terminating section of the Greenland Ice Sheet, Earth System Science Data, 6:331-338, doi:10.5194/essd-6-331-2014.

Jakobsson, M., L. A. Mayer, C. Bringensparr, C. F. Castro, R. Mohammad, P. Johnson, T. Ketter, D. Accettella, D. Amblas, L. An, J. E. Arndt, M. Canals, J. L. Casamor, N. Chauché, B. Coakley, S. Danielson, M. Demarte, M. Dickson, B. Dorschel, J. A. Dowdeswell, S. Dreutter, A. C. Fremand, D. Gallant, J. K. Hall, L. Hehemann, H. Hodnesdal, J. Hong, R. Ivaldi, E. Kane, I. Klaucke, D. W. Krawczyk, Y. Kristoffersen, B. R. Kuipers, R. Millan, G. Masetti, M. Morlighem, R. Noormets, M. M. Prescott, M. Rebesco, E. Rignot, I. Semiletov, A. J. Tate, P. Travaglini, I. Velicogna, P. Weatherall, W. Weinrebe, J. K. Willis, M. Wood, Y. Zarayskaya, T. Zhang, et al. 2020. The international bathymetric chart of the arctic ocean version 4.0. Nature Sci. Data., 7(1):176.

Jansen, D., S. Franke, T. Binder, V.Helm, J. D. Paden. 2020. Ice thickness from the northern catchment region of Greenland's 79 North Glacier, recorded with the airborne AWI UWB radar system. Alfred Wegener Institute, Helmholtz Centre for Polar and Marine Research, Bremerhaven, PANGAEA, doi:10.1594/PANGAEA.913193.

Kjær, K. H., N. K. Larsen, T. Binder, A. A. Bjørk, O. Eisen, M. A. Fahnestock, S. Funder, A. A. Garde, H. Haack, V. Helm, M. Houmark-Nielsen, K. K. Kjeldsen, S. A. Khan, H. Machguth, I. McDonald, M. Morlighem, J. Mouginot, J. D. Paden, T. E. Waight, C. Weikusat, E. Willerslev, and J. A. MacGregor. 2018. A large impact crater beneath Hiawatha Glacier in northwest Greenland. Sci. Adv., 4(11), doi:10.1126/sciadv.aar8173.

Millan, R., E. Rignot, J. Mouginot, M. Wood, A. A. Bjørk, and M. Morlighem. 2018. Vulnerability of southeast Greenland glaciers to warm Atlantic water from Operation IceBridge and Ocean Melting Greenland data. Geophys. Res. Lett., 45(6):2688–2696, doi:10.1002/2017GL076561.

Mix, A. C., M. Jakobsson, and the Petermann-2015 Scientific Party. 2015. Petermann-2015 Expedition Launches International Collaboration in Arctic Science, Tech. rep., Arctic Research Consortium of the United States.

Morlighem M. et al. 2017. BedMachine v3: Complete bed topography and ocean bathymetry mapping of Greenland from multi-beam echo sounding combined with mass conservation, Geophys. Res. Lett., 44, doi:10.1002/2017GL074954. (http://onlinelibrary.wiley.com/doi/10.1002/2017GL074954/full)

Morlighem, M., E. Rignot, and J. Willis. 2016b. Improving bed topography mapping of Greenland glaciers using NASA's Oceans Melting Greenland (OMG) data, Oceanography, 29.

Morlighem, M., E. Rignot, J. Mouginot, H. Seroussi and E. Larour. 2014. Deeply incised submarine glacial valleys beneath the Greenland Ice Sheet, Nature Geoscience, 7:418-422. doi:10.1038/ngeo2167.

Morlighem, M, E. Rignot, J Mouginot, H. Seroussi, and E. Larour. 2014. High-resolution ice thickness mapping in South Greenland. Annals of Glaciology, 55(67):1–7.

Morlighem, M, E. Rignot, J. Mouginot, X. Wu, H. Seroussi, E. Larour, and J. Paden. 2013. High-resolution bed topography mapping of Russell Glacier, Greenland, inferred from Operation IceBridge data. Journal of Glaciology, 59(218):1015–1023.

Morlighem, M, E. Rignot, H. Seroussi, E. Larour, H. Ben Dhia, and D. Aubry. 2011. A mass conservation approach for mapping glacier ice thickness. Geophysical Research Letters, 38(L19503):1–6.

Motyka, R. J., R. Cassotto, M. Truffer, K. K. Kjeldsen, D. Van As, N. J. Korsgaard, M. Fahnestock, I. Howat, P. L. Langen, J. Mortensen, , K. Lennert, and S. Rys- gaard. 2017. Asynchronous behavior of outlet glaciers feeding Godthåbsfjord (NuupKangerlua) and the triggering of Narsap Sermia's retreat in SW Greenland, J. Glaciol., 63(238), 288308, doi:10.1017/jog.2016.138.

Mouginot, J., E. Rignot, B. Scheuchl, and R. Millan. 2017. Comprehensive Annual Ice Sheet Velocity Mapping Using Landsat-8, Sentinel-1, and RADARSAT-2 Data, Remote Sens., 9(4), doi:10.3390/rs9040364.

Nixdorf, U., D. Steinhage, U. Meyer, L. Hempel, M. Jenett, P. Wachs, and H. Miller. 1999. The newly developed airborne radio-echo sounding system of the AWI as a glaciological tool, Ann. Glaciol., 29, 231–238, doi:10.3189/172756499781821346

Noël, B., W. J. van de Berg, H. Machguth, S. Lhermitte, I. Howat, X. Fettweis, and M. R. van den Broeke. 2016. A daily, 1 km resolution data set of downscaled Greenland ice sheet surface mass balance (1958–2015), Cryosphere, 10(5), 2361–2377, doi:10.5194/tc-10-2361-2016.

O'Cofaigh, C., J. A. Dowdeswell, A. E. Jennings, K. A. Hogan, A. Kilfeather, J. F. Hiem- stra, R. Noormets, J. Evans, D. J. McCarthy, J. T. Andrews, J. M. Lloyd, and M. Moros. 2013. An extensive and dynamic ice sheet on the West Greenland shelf during the last glacial cycle, Geology, 41(2), 219–222.

OMG Mission. 2016. Bathymetry (sea floor depth) data from the ship-based bathymetry survey. Ver. 0.1. OMG SDS, CA, USA http://dx.doi.org/10.5067/OMGEV-BTYSS.

OMG Mission. 2020. Bathymetry (sea floor depth) data from the ship-based bathymetry survey. Ver. 0.1. OMG SDS, CA, USA. Dataset accessed 2020-01-01 at https://dx.doi.org/10.5067/OMGEV-BTYSS.

Peters, M., D. Blankenship, and D. Morse. 2005. Analysis techniques for coherent air- borne radar sounding: Application to West Antarctic ice streams, J. Geophys. Res., 110(B6), doi:10.1029/2004JB003222.

Peters, M. E., D. D. Blankenship, S. P. Carter, S. D. Kempf, D. A. Young, and J. W. Holt. 2007. Along-track focusing of airborne radar sounding data from West Antarctica for improving basal reflection analysis and layer detection, IEEE Trans. Geosc. and Rem.Sens., 45(9), 2725–2736, doi:10.1109/TGRS.2007.897416.

Raney, K. 2010. IceBridge PARIS L2 ice thickness. version 1.0, doi: 10.5067/OMEAKG6GIJNB, Boulder, Colorado USA: NASA DAAC at the National Snow and Ice Data Center

Rignot, E. and J. Mouginot. 2012. Ice flow in Greenland for the International Polar Year 2008–2009. Geophysical Research Letters, 39:L11501.

Rignot, E., I. Fenty, Y. Xu, C. Cai, and C. Kemp. 2015. Undercutting of marine-terminating glaciers in West Greenland, Geophys. Res. Lett., 42(14), 5909–5917, doi:10.1002/2015GL064236.

Rignot, E., I. Fenty, Y. Xu, C. Cai, I. Velicogna, C. O'Cofaigh, J. A. Dowdeswell, W. Weinrebe, G. Catania, and D. Duncan. 2016. Bathymetry data reveal glaciers vulnerable to ice-ocean interaction in Uummannaq and Vaigat glacial fjords, west Greenland, Geophys. Res. Lett., 43(6), 2667–2674.

Rysgaard, S., T. Vang, M. Stjernholm, B. Rasmussen, A. Windelin, and S. Kiilsholm. 2003. Physical conditions, carbon transport, and climate change impacts in a northeast Greenland fjord, Arctic Ant. Alp. Res., 35(3), 301–312, doi:10.1657/1523- 0430(2003)035[0301:PCCTAC]2.0.CO;2.

Schaffer, J., R. Timmermann, J. E. Arndt, S. S. Kristensen, C. Mayer, M. Morlighem, and D. Steinhage. 2016. A global, high-resolution data set of ice sheet topography, cavity geometry, and ocean bathymetry, Earth Syst. Sci. Data, 8(2), 543–557, doi:10.5194/essd- 8-543-2016.

Schenk, T. and B. A. Csatho, B. 2012. A new methodology for detecting ice sheet surface elevation changes from laser altimetry data. IEEE Transactions on Geoscience and Remote Sensing, 50:3302–3316.

Schumann, K., D. Voelker, and W. R. Weinrebe. 2012. Acoustic mapping of the Ilulissat Ice Fjord mouth, West Greenland, Quat. Sci. Rev., 40, 78–88.

Slabon, P., B. Dorschel, W. Jokat, R. Myklebust, D. Hebbeln, and C. Gebhardt. 2016. Greenland ice sheet retreat history in the northeast Baffin Bay based on high-resolution bathymetry, Quat. Sci. Rev., 154, 182 – 198, doi: http://doi.org/10.1016/j.quascirev.2016.10.022.

Sørensen, L. S., S. B. Simonsen, R. Forsberg, L. Stenseng, H. Skourup, S. S. Kristensen, and W. Colgan. 2019. Programme for monitoring of the Greenland ice sheet (PROMICE): Airborne survey. Dataset published via Geological Survey of Denmark and Greenland and DTU-Space, doi:10.22008/promice/data/airbornesurvey

Stevens, L. A., F. Straneo, S. B. Das, A. J. Plueddemann, A. L. Kukulya, and M. Morlighem. 2016. Linking glacially modified waters to catchment-scale subglacial discharge using autonomous underwater vehicle observations, Cryosphere, 10(1), 417– 432, doi:10.5194/tc-10-417-2016.

Straneo, F., D. A. Sutherland, D. Holland, C. Gladish, G. S. Hamilton, H. L. Johnson, E. Rignot, Y. Xu, and M. Koppes. 2012. Characteristics of ocean waters reaching Greenland’s glaciers, Ann. Glaciol., 53(60, 2), 202–210.

Straneo, F., G. S. Hamilton, L. A. Stearns, and D. A. Sutherland. 2016. Connecting the Greenland Ice Sheet and the Ocean, a case study of Helheim Glacier and Sermilik Fjord, Oceanography, 29(4, SI), 34–45.

Sutherland, D. A., F. Straneo, and R. S. Pickart. 2014. Characteristics and dynamics of two major Greenland glacial fjords, J. Geophys. Res. - Oceans, 119(6), 3767–3791.

Sutherland, D. A., and R. S. Pickart. 2008. The East Greenland Coastal Current: Structure, variability, and forcing, Prog. Oceanogr., 78(1), 58–77, doi: 10.1016/j.pocean.2007.09.006.

Thomsen, H., et al. 1997. The Nioghalvfjerdsfjorden glacier project, north-east Greenland: a study of ice sheet response to climatic change, Geology of Greenland Survey Bulletin, 179:95.

Weinrebe, R. W., A. KuijpKui, I. Klaucke, and M. Fink. 2009. Multibeam Bathymetry Surveys in Fjords and Coastal Areas of West-Greenland, in Eos Trans. AGU, 90(52), Fall Meet. Suppl., Abstract OS21A1152.

4.1 Related Data Collections

- IceBridge MCoRDS L2 Ice Thickness

4.2 Related Websites

- Ice Sheet Modeling Group, Department of Earth System Science, University of California Irvine (http://sites.uci.edu/morlighem/)

5 CONTACTS AND ACKNOWLDGMENTS

5.1 Contacts

Mathieu Morlighem

Department of Earth System Science

University of California, Irvine

Irvine CA, 92617, USA

5.2 Acknowledgments

This work was performed at the University of California Irvine under a contract with the NASA Cryospheric Sciences Program (#NNX15AD55G), and the National Science Foundation's ARCSS program (#1504230), and in cooperation with the University of Bristol as part of the Basal Properties of Greenland project (NERC grant NE/M000869/1).

We would like to thank GRISO RCN (Greenland Ice Sheet Ocean Research Coordination Network) for their help in finding available bathymetry data.

6 DOCUMENT INFORMATION

6.1 Publication Date

June 2021

6.2 Date Last Updated

1 August 2022